Carbon stable isotope records in the coral species *Siderastrea stellata*: a link to the Suess Effect in the tropical South Atlantic Ocean

N.S. Pereira[1,2*], A.N. Sial[1], S.-C. Liu[3], C.-C. Shen[3], C. V. Ullmann[4], R. Frei[5], C. Korte[5], R.K.P. Kikuchi[6], V.P. Ferreira[2], K. H. Kilbourne[7], B.L.S. Braga[6].

[1]*NESP, Department of Biology, State University of Bahia, Campus VIII, Paulo Afonso, 48608-240, Brazil.*

[2]*NEG-LABISE, Federal University of Pernambuco, C. P. 7852, Recife, 50670-000, Brazil.*

[3]*High-Precision Mass Spectrometry and Environment Change Laboratory (HISPEC), Department of Geosciences, National Taiwan University, Roosevelt Rd., Taipei 10617, Taiwan, ROC.*

[4]*University of Exeter, Camborne School of Mines, Penryn Campus, Treliever Road, Penryn, Cornwall, TR10 9FE, UK.*

[5] *Department of Geosciences and Natural Resource Management & Nordic Center for Earth Evolution (NordCEE), University of Copenhagen, Øster Voldgade 10, 1350 Copenhagen, Denmark.*

[6] *RECOR, Department of Oceanography, Federal University of Bahia, Salvador, 40210-340, Brazil.*

[7]*Chesapeake Biological Laboratory, Maryland University, 146 Williams Street, P.O. Box 38 Solomons, MD 20688.*

Abstract

Coral skeletons are natural archives whose geochemical signatures provide insights into the tropical ocean history beyond the instrumental record. Carbon stable isotopes from coral skeletons ($\delta^{13}C_{coral}$) have been used as a proxy for multiple variables on a seasonal basis. Long-term changes in coral $\delta^{13}C$ relate to the changing isotopic composition of the dissolved inorganic carbon ($\delta^{13}C_{DIC}$). $\delta^{13}C_{DIC}$ in turn reflects changes in the $\delta^{13}C$ of atmospheric CO_2, which in the modern Earth system is governed primarily by anthropogenic injection of CO_2 into the atmosphere – a process known as the Suess Effect.

Here we report three $\delta^{13}C$ coral-based records of *Siderastrea stellata* from the tropical South Atlantic. U-series dating for the colonies 12SFB-1, 13SS-1 and 13SS-2 suggests these corals lived 13, 57 and 65 years, respectively. Short-term $\delta^{13}C$ variations in their skeletal aragonite are dominated by inter-annual variation. All three $\delta^{13}C$ records additionally exhibit an overall decreasing trend, with a depletion of about -0.0243 ± 0.0057 ‰.yr^{-1} (12SFB-1), -0.0208 ± 0.0007 ‰.yr^{-1} (13SS-1) and -0.0214 ± 0.0013 ‰.yr^{-1} (13SS-2). These rates of the coral records from Rocas Atoll are similar to the reported trend for the $\delta^{13}C$ of atmospheric CO_2 over the years 1960-1990 (-0.023 to -0.029 ‰.yr^{-1}), and to the estimated decreasing rates of global $\delta^{13}C_{DIC}$.

Our findings suggest that multiple $\delta^{13}C$ coral-based records are required for confidently identifying local changes in the $\delta^{13}C_{DIC}$ of the ocean. This information, in turn, can be used to infer changes in the $\delta^{13}C$ of the atmospheric CO_2 composition and provide valuable information about recent changes on the carbon biogeochemical cycle during the Anthropocene epoch.

Keywords: Coral geochemistry; Climate changes; CO_2; Coral-based archives

*Corresponding author: Natan S. Pereira; e-mail: nspereira@uneb.br
phone: 55-81-2126-8243

1. Introduction

Scleractinian corals incorporate geochemical signatures in their exoskeleton that can be used to reconstruct the environmental history of the tropical oceans (e.g., Weber and Woodhead 1970; Weber 1973; Swart 1983; Swart and Grottoli 2003). The suitability of corals to act as climate archives relies on high-quality calibrations of modern coral skeletal chemistry (stable isotopes, as well as trace and minor elements) that can be applied in ancient corals (e.g., Linsley et al. 1994; Corrège 2006; DeLong et al. 2007, 2013). Such environmental reconstructions in turn improve our knowledge about past climate parameters beyond the instrumental record.

Some geochemical proxies are well established in coral records, such as $\delta^{18}O$ values and Sr/Ca ratios for tracking sea surface temperature (SST) (e.g. Weber and Woodhead 1970, 1972; Weber 1973; Swart 1983b; Leder et al. 1996; Felis et al. 2000; Guilderson et al. 2001; Swart et al. 2002; Moses et al. 2006; DeLong et al. 2011). The meaning of coral $\delta^{13}C$, however, still remains incompletely understood due to the multitude of physiological and environmental parameters involved (Swart 1983a; McConnaughey 1989a, 1989b, 2003; Swart et al. 1996; Al-Rousan and Felis 2013).

The C and O isotopic composition of corals is depleted compared aragonite formed in isotopic equilibrium with seawater due to kinetic and metabolic fractionation (Weber and Woodhead 1970). Carbon used corals for the secretion of their aragonite skeleton is sourced from CO_2 which diffuses across the boundary membranes and ionizes to form non-diffusible HCO_3^- and CO_3^{2-}. The latter combine with Ca^{2+} in the calcifying space to form $CaCO_3$. Depleted $\delta^{13}C$ and $\delta^{18}O$ values in the resulting carbonate are a function of kinetic fractionation during CO_2 hydration and hydroxylation (McConnaughey 1989a).

It has been suggested that the intra-annual variations of $\delta^{13}C$ are caused by photosynthetic activity by the host symbionts (the zooxanthellae), which would change the carbon isotopic composition of the internal dissolved inorganic carbon (DIC) pool from which coral aragonite forms (e.g. Fairbanks and Dodge 1979; Pätzold 1984; Grottoli and Wellington 1999). Increases in the rate of photosynthesis due to increased solar irradiance have been observed to parallel increases in the coral $\delta^{13}C$, while a reduction in solar irradiance led to depleted $\delta^{13}C$ values (Weber and Woodhead 1970). Consequently, carbon isotope ratios in corals could be used as a proxy for solar irradiance or cloud coverage (Fairbanks and Dodge 1979; Pätzold 1984; Grottoli and Wellington 1999; Sun et al. 2008, among others).

However, many studies have shown a range of additional factors that may play significant roles in the seasonal variations of coral $\delta^{13}C$. Amongst these are water depth (e.g., Fairbanks and Dodge 1979; Swart et al. 1996; Grottoli and Wellington 1999), heterotrophic level (Grottoli and Wellington 1999), kinetic isotope fractionation (McConnaughey 1989b), reproduction (Gagan et al. 1994), bleaching (Leder et al. 1991), spawning (Gagan et al. 1994) and the $\delta^{13}C$ of regional DIC (Swart et al. 2010; Al-Rousan and Felis 2013; Dassié et al. 2013; Deng et al. 2017) .

Beyond the complicated short-term variations in coral $\delta^{13}C$, decadal- to centennial-scale changes in coral $\delta^{13}C$ are observed and related to modifications of the $\delta^{13}C$ of the surface water DIC (Swart et al. 1996, 2010; Al-Rousan and Felis 2013; Dassié et al. 2013; Deng et al. 2017). Long-term decreases in coral $\delta^{13}C$ have first been reported as early as the 1970s (Nozaki et al. 1978). This trend was first attributed to the Suess Effect by Druffel and Benavides (1986) and has been since reported in coral-based records from the Pacific ocean, Indian ocean, Red Sea, North Atlantic ocean and Caribbean Sea (Swart et al. 2010; Al-Rousan and Felis 2013; Dassié et al. 2013 and references therein).

Changing $\delta^{13}C$ of atmospheric CO_2 since the industrial revolution caused by anthropogenic CO_2 input to the atmosphere from fossil fuel burning and deforestation has become widely known as the Suess Effect (Keeling 1979). Because anthropogenic CO_2 has a distinctly negative $\delta^{13}C$ signature of about −28‰ (Andres et al. 2013), this change has been to progressively more negative atmospheric $\delta^{13}C$, amounting to about 1.14‰ since the beginning of the industrial revolution according to carbon isotopic data retrieved from air bubbles trapped in ice cores (Friedli et al. 1986). 30 to 40% of the anthropogenic CO_2 influx is currently taken-up by the oceans (Quay et al. 1992; Orr et al. 2001) which caused $\delta^{13}C$ of the DIC reservoir to decrease in parallel to the atmosphere through the last two centuries (Al-Rousan and Felis 2013).

Here we report three coral-based $\delta^{13}C$ records for the Tropical South Atlantic Ocean retrieved from colonies of the hermatypic massive coral *Siderastrea stellata*. *S. stellata* represents one the of the main reef builders of the Brazilian reefs, with a spatial distribution from 0° to 23°S (Lins-de-Barros and Pires 2007). Evaluating the potential of this species as a climate archive in the South Atlantic Ocean is importnat, because it is widespread on Brazilian reefs and relatively abundant compared to other species. In this study, we explore possible explanations for the short and long-term variability on the $\delta^{13}C$ signature on the *S. stellata* skeleton.

2. Study area

The Rocas Atoll (3°51´S, 33°49´W) is the only atoll in the western part of the South Atlantic, 266 km offshore from the city of Natal, northeastern Brazil (Fig. 1). Because of its isolated location the Rocas Atoll receives no direct terrestrial input. This locality constitutes a natural laboratory where ocean and atmospheric processes are the key players, allowing for near-pristine geochemical signatures in biogenic carbonates. At this peculiar atoll, most corals live in tidal pools which are under influence of a semi-diurnal

and mesotidal regime, with a maximum tidal range of 3.8 m (Gherardi and Bosence 2001). The physicochemical, geologic and oceanographic conditions of the Rocas Atoll are described by Kikuchi and Leão (1997) and Pereira et al. (2013).

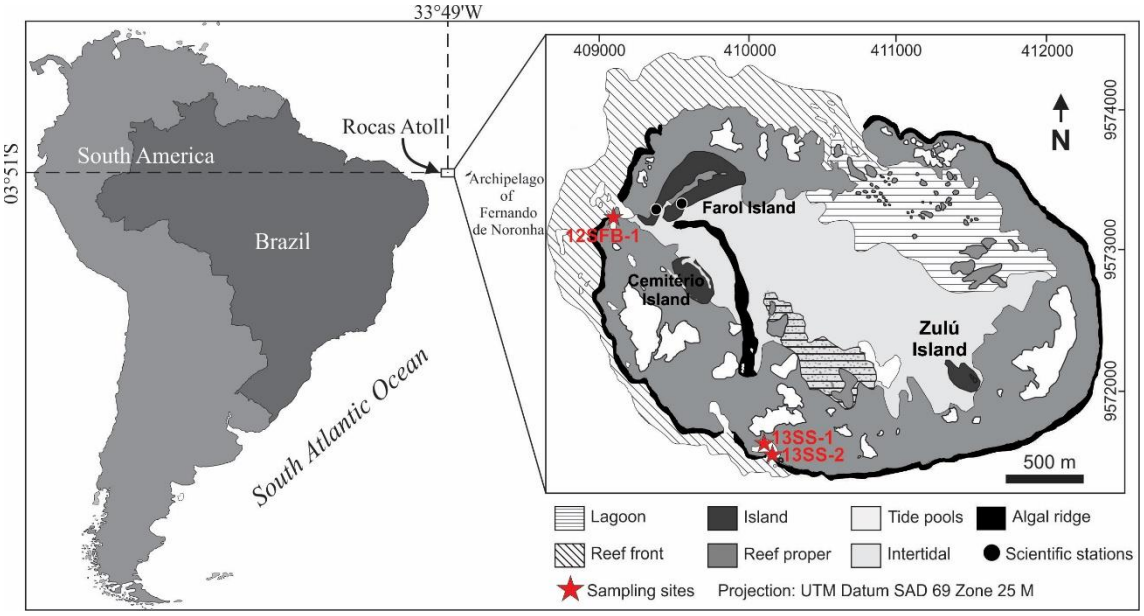

Figure 1. Location and geomorphological map of the reef complex of Rocas Atoll, with indicated sampling site (red stars) for the colonies 12SFB-1, 13SS-1 and 13SS-2. Modified from (Pereira et al 2010).

3. Methodology

3.1. Studied colonies

For this study, three colonies of *S. stellata* were used. Colonies 13SS-1 and 13SS-2, both with approximately 50-cm diameter, were collected at the south portion of the atoll (Fig. 1), from about 7 m depth, in July 2013. The colony 12SFB-1, a 15-cm diameter colony, was collected dead, but still attached to the reef substrate, at the northwestern part of the Rocas Atoll, at 3 m depth in January of 2012 (Fig. 1).

3.2. Sampling for geochemical analysis

The studied colonies were cut into halves, and one half was cut into 5-mm thick slices, parallel to the growth axis of the whole colony. After cutting, these slices were cleaned with deionized water, air-dried and then X-rayed at 50 kV and 320 mA, with an

exposure time of 3.2 s and distance from the equipment to the object of 108 cm. Carbonate samples were collected at 0.5 mm intervals using a micromill (the section from 150-188 of coral 13SS-1 was sampled with 1 mm resolution). The coral powder was produced by continuous, progressive grinding of the slab from the top towards the bottom, following the thecal wall (Fig. 2).

Additional samples were collected along the growth axis of each colony (Fig. 2) for dating by a high precision ^{230}Th method (Shen et al. 2008b, 2012). Eleven subsamples, 0.10-0.25 g each, were cut from three corals (Fig. 2) for U-Th dating. They were gently crushed, physically cleaned with ultrasonic methods, and dried for U-Th chemistry.

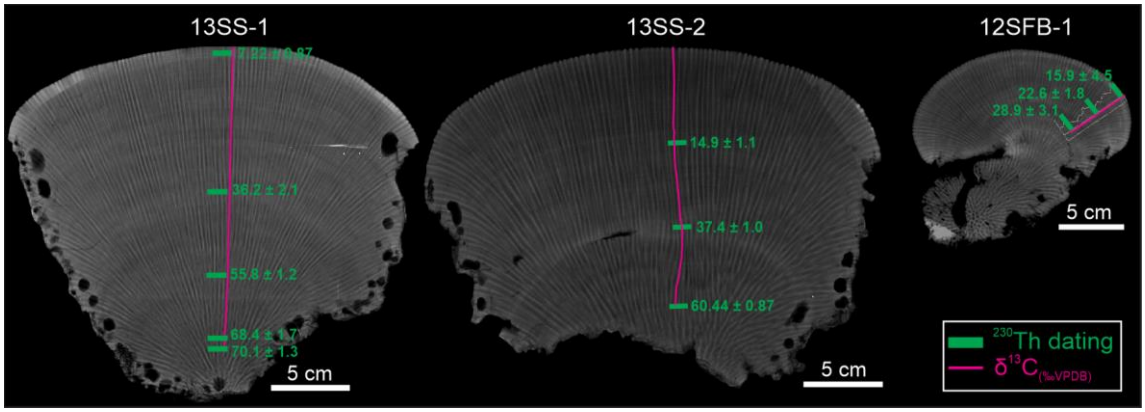

Figure 2. Radiographies of 5-mm-thick slices of the 13SS-1, 13SS-2 and 12SFB-1 coral colonies. Density bands are not annual in the X-radiographs, inhibiting age assignment by band counting alone. The sections analyzed for δ^{13}C (purple line) followed a single corallite wall track. Subsamples along the coral slab of each colony were collected for U-Th dating (green bars), numbers reported in green represent years before 11th July, 2016 for the colonies 13SS-1 and 12SFB-1, and before 1st January, 2016.

3.3. Geochemical analyses

3.3.1. Carbon and oxygen stable isotope

All coral δ^{13}C and δ^{18}O data are reported in per mill relative to VPDB. Colony 13SS-2 and 12SFB-1 were measured at the Federal University of Pernambuco using a Delta V Advantage coupled with a GasBench II device. Sets containing 56 coral samples

were analyzed against 16 samples of 4 different standards, 2 international, NBS-18 and NBS-19 and 2 internal, REI and VICKS (n = 128). The precision of the analysis was better than 0.1 ‰ for $\delta^{13}C$ and $\delta^{18}O$, except for $\delta^{18}O$ of colony 13SS-2, which are affected by analytical issues and will not be presented here.

$\delta^{13}C$ values for coral carbonate samples of the colony 13SS-1 were analyzed at the University of Copenhagen, using a Micromass IsoPrime mass spectrometer, employing the protocols adopted from Spötl and Vennemann (2003) with modifications described in Ullmann et al. (2013). The precision of the method was assessed by multiple measurements of the laboratory reference material LEO (Carrara Marble) and was 0.09 ‰ for $\delta^{13}C$ and 0.10 ‰ for $\delta^{18}O$ (2σ, n = 129).

3.3.2. Sr/Ca ratios

Coral Sr/Ca ratios were measured using a Perkin Elmer Optima 7000 DV ICP-OES at the University of Copenhagen. The samples were measured at a Ca concentration of ~10 µg/g against a synthetic calibration solution. The calibration solution contained only Ca and Sr with a Sr/Ca ratio of 9.1289 mmol/mol. The measurements were done on the 317.933 nm line of Ca and the 407.771 nm line of Sr. Accuracy was controlled using JLs-1, for which Sr/Ca ratios reproduced to 1.6 % (2 rsd) at a value of 0.345 mmol/mol (n = 83). All samples were analyzed at least twice and average repeatability of the Sr/Ca ratio is 0.6 % (2 err). The measured values for Sr/Ca in JLs-1 are within 1 % of the values computed from Imai et al. (1996).

3.4. U/Th dating and age model

Coral skeletal density patterns revealed by x-radiographies are often useful for accurate chronologic control (Knutson et al. 1972). The density patterns of the *S. stellata*

specimens in this study, however, are not distinct. Thus, this methodology is not appropriate for determining the age of these corals. To construct a reliable age model for these colonies, we applied ^{230}Th dating through the profile section where δ^{13}C was retrieved.

U-series dating was conducted in a class-10.000 metal-free clean room with class-100 benches at the High-Precision Mass Spectrometry and Environment Change Laboratory (HISPEC), Department of Geosciences, National Taiwan University (Shen et al. 2008a). U-Th isotopic compositions and concentrations were determined on a multi-collector inductively-coupled plasma mass spectrometer (MC-ICP-MS) in the HISPEC (Shen et al. 2012). Half-lives of U-Th nuclides used for ^{230}Th age calculation are given in (Cheng et al. 2013). Uncertainties in the U-Th isotopic data and ^{230}Th dates are calculated at the 2σ level or two standard deviations of the mean ($2\sigma_m$) unless otherwise noted.

An age model for each core was constructed based on linearly interpolating between the uranium series dates and linearly extending the growth estimates in the short skeletal sections not bounded by radiometric dates.

3.5. Growth rate

The U-series dates enable the calculation of average growth rates by dividing the recorded time interval (years) by the total length (mm) of the coral record. Growth rate was also determined for the various sub-sections bracketed by ^{230}Th date samples in each coral record, by dividing the record span (years) by the extension (mm) of each of these sub-section.

3.6. Fourier transform analyses

A Fourier transformation of the data was conducted on the depth series data before age modeling to explore the variance of the data in frequency space. For the spectral analysis, evenly sampled data (0.5 mm/sample) were de-trended before applying a standard Blackman Tukey correlogram analysis with a Bartlet window using the SSA-MTM toolkit (Dettinger et al. 1995; Ghil et al. 2002).

4. Results

4.1. U/Th chronology

Determined U-Th isotopic compositions and ^{230}Th dates are listed in Table 1. U-Th dating of subsamples retrieved along the growth axis of the colony 13SS-1 (n = 4, Fig. 3) constrained the geochemical record to the years 1948-2013. (Fig. 3). For the colony 13SS-2 (n = 3), U-Th dating points to a recorded interval from 1956 to 2013 and for the colony 12SFB-1 (n = 3), a sampled interval from 1988 to 2001 (Fig. 3).

Many coral records have particularly clear seasonal δ^{13}C cycles, but no straightforward evaluation of seasonal signals in the present specimens is possible. Apparent cycles in the 13SS-1 and 13SS-2 records (Fig. 3) are demonstrated by the U-series age not to be annual. In contrast to many other coral specimens, δ^{13}C cycles can therefore not be used to refine the age model of this coral. In the coral 12SFB-1 on the other hand the number of cycles agrees with the U-series age (Table 2). The contrasting ages between ^{230}Th and the number of δ^{13}C cycles in 13SS-1 and 13SS-2 indicates: (i) possible hiati in coral growth, or (ii) that high frequency cycles of the δ^{13}C signal are dominated by inter-annual variability rather than seasonal variability.

The number of δ^{13}C cycles (poorly defined) at the youngest part of the coral records 13SS-1 and 13SS-2 is compatible with U-series ages. Throughout ontogeny, however, the number of δ^{13}C cycles increasingly disagree with U-series ages (table 2). Given that the

skeleton seems to show continuous growth (except in the coral 13SS-2 just before the 1979 date, where it is possible to see a slightly denser band and the die-off of a small section of the coral; see Fig. 3), a likely explanation is that these are not seasonal cycles. Rocas Atoll is close to the equator where there is very little seasonality, whereas inter-annual variability of climate parameters may be more important.

234 **Table 1. U-Th isotopic compositions and ^{230}Th ages for coral samples by MC-ICPMS at HISPEC, NTU†.**

Colony	Sample ID	Weight g	^{238}U ng/g[a]	^{232}Th pg/g	δ^{234}U measured[a]	[^{230}Th/^{238}U] activity (x 10^{-6})[c]	[^{230}Th/^{232}Th] atomic (x 10^{-6})	Age uncorrected	Age corrected [c,d]	$\delta^{234}U_{initial}$ corrected[b]
13SS-1	SS1-1.1	0.13840	2918.4 ± 4.6	172.0 ± 3.4	143.0 ± 2.5	90.0 ± 5.6	25.2 ± 1.6	8.58 ± 0.54	7.22 ± 0.87	143.0 ± 2.5
	SS1-2.1	0.14800	2927.4 ± 5.6	478.9 ± 3.3	146.2 ± 2.5	419.8 ± 9.0	42.31 ± 0.95	39.94 ± 0.86	36.2 ± 2.1	146.3 ± 2.5
	SS1-3.1	0.17620	2832.2 ± 4.5	58.1 ± 2.6	143.1 ± 2.4	590 ± 13	474 ± 24	56.3 ± 1.2	55.8 ± 1.2	143.1 ± 2.4
	SS1-4.X	0.10780	2861.9 ± 5.2	289.1 ± 4.3	141.8 ± 2.5	741 ± 12	120.9 ± 2.7	70.7 ± 1.2	68.4 ± 1.7	141.8 ± 2.5
12SFB-1	SFB-1	0.18980	3299.1 ± 3.8	1260.4 ± 4.0	144.7 ± 1.9	259 ± 11	11.18 ± 0.46	24.7 ± 1.0	15.9 ± 4.5	144.7 ± 1.9
	SFB-2	0.13840	3173.7 ± 4.0	462.1 ± 3.4	145.1 ± 1.9	273.1 ± 7.2	30.92 ± 0.84	26.00 ± 0.68	22.6 ± 1.8	145.2 ± 1.9
	SFB-3	0.11500	3140.6 ± 4.0	812.6 ± 4.3	147.4 ± 1.8	367.3 ± 8.7	23.41 ± 0.56	34.92 ± 0.82	28.9 ± 3.1	147.4 ± 1.8
13SS-2	SS2-1	0.18150	2558.4 ± 2.4	224.8 ± 2.6	144.9 ± 1.7	177.5 ± 4.7	33.29 ± 0.97	16.90 ± 0.45	14.9 ± 1.1	144.9 ± 1.7
	SS2-2	0.22665	2649.9 ± 2.8	175.0 ± 2.1	144.7 ± 1.8	408.8 ± 6.7	102.1 ± 2.1	38.95 ± 0.64	37.4 ± 1.0	144.8 ± 1.8
	SS2-3	0.24368	2869.0 ± 2.6	152.1 ± 1.9	141.3 ± 1.6	645.2 ± 6.4	200.7 ± 3.2	61.67 ± 0.62	60.4 ± 0.9	141.3 ± 1.6

235 †Analytical errors are 2σ of the mean.

236 [a] $[^{238}U] = [^{235}U] \times 137.77$ (±0.11‰) (Hiess et al., 2012); $\delta^{234}U = ([^{234}U/^{238}U]_{activity} - 1) \times 1000$.

237 [b] $\delta^{234}U_{initial}$ corrected was calculated based on ^{230}Th age (T), i.e., $\delta^{234}U_{initial} = \delta^{234}U_{measured} \, X \, e^{\lambda 234 * T}$, and T is corrected age.

238 [c] $[^{230}Th/^{238}U]_{activity} = 1 - e^{-\lambda 230 T} + (\delta^{234}U_{measured}/1000)[\lambda_{230}/(\lambda_{230} - \lambda_{234})](1 - e^{-(\lambda 230 - \lambda 234) T})$, where *T* is the age. Decay constants are 9.1705×10^{-6} yr^{-1} for ^{230}Th, 2.8221×10^{-6} yr^{-1} for ^{234}U (Cheng et al., 2013), and 1.55125×10^{-10} yr^{-1} for ^{238}U (Jaffey et al., 1971).

240 [d] The degree of detrital ^{230}Th contamination is indicated by the [^{230}Th/^{232}Th] atomic ratio instead of the activity ratio.

241 [e] Age corrections, relative to chemistry date on 1th, January, 2016 (colony 13SS-2) and 11th, July, 2016 (colonies 12SFB-1 and 13SS-1), were calculated using an estimated
242 atomic ^{230}Th/^{232}Th ratio of 4 ± 2 ppm (Shen et al., 2008)

4.2. Growth rate

The mean growth rates for the studied colonies estimated by U-series data revealed values of 2.75 ± 0.65 mm.year^{-1} for 13SS-1, 3.18 ± 2.09 mm.year^{-1} for 13SS-2 and 3.45 ± 0.40 mm.year^{-1} for 12SFB-1 (table 2). Therefore, the growth rate of theses specimens are not constant through time but vary from 1.85 to 3.41 mm.year^{-1} for colony 13SS-1, 1.74 to 5.57 mm.year^{-1} for colony 13SS-2, and 3.17 to 3.73 mm.year^{-1} (Table 2).

The coral 13SS-2 showed the highest growth rate (5.57 mm.year^{-1}) that decreases to much slower rates (1.74 to 2.22 mm.year^{-1}) in older sections. An opposite behavior, however, is observed for colony 13SS-1, in which growth rate is higher (3.41 mm.year^{-1}) in older sections and decreases to slower rates at the youngest part (1.85 mm.year^{-1}). Colony 12SFB-1 presented constant values through the record.

Table 2. Comparisons of age and growth based on $\delta^{13}C$ cycles and U-series dates.

Colony	Sample ID	Depth range (mm)	Age interval (U-series)	Growth rate (mm.y^{-1})	$\delta^{13}C$ cycles	Years (U-series)
13SS-1	SS1-1.1	0-8	2009-2013*	1.85	1	4
	SS1-2.1	8 to 90	1980-2009	2.83	18	29
	SS1-3.1	90 to 147	1961-1980	2.91	14	20
	SS1-4.X	147 to 190	1948-1961	3.41	5	13
				****2.75 ± 0.65**		
13SS-2	SA1	0 to 70	2001-2013*	5.57	15	13
	SA2	70 to 120	1979-2001	2.22	12	23
	SA3	120 to 160	1956-1979	1.74	11	23
				****3.18 ± 2.09**		
12SFB-1	SFB2	5 to 30	1994-2001	3.73	7	7
	SFB3	30 to 50	1988-1994	3.17	6	6
				****3.45 ± 0.40**		

*Growth rate and calendar years calculated from October/2013. **Mean growth rate estimated on basis of U-series age for the total coral record.

4.1. Carbon stable isotopes data ($\delta^{13}C$)

The coral $\delta^{13}C$ values range from −1.92 to +0.58‰, with a mean value of −0.76 ± 0.45‰ and variance of 0.20‰ in colony 13SS-1 (n = 325). Colony 13SS-2 $\delta^{13}C$ values range from −2.06 to 0.51‰, with a mean value of −0.75 ± 0.55‰ and variance of 0.3‰

(n = 312). The carbon isotopic composition of colony 12SFB-1 varied from −1.19 to +0.13‰, with a mean value of −0.54 ± 0.26‰ and variance of 0.07‰ (n = 95).

All three $\delta^{13}C$ profiles are characterized by consistent decreasing trends from the oldest towards more recently formed skeletal material (Fig. 3).

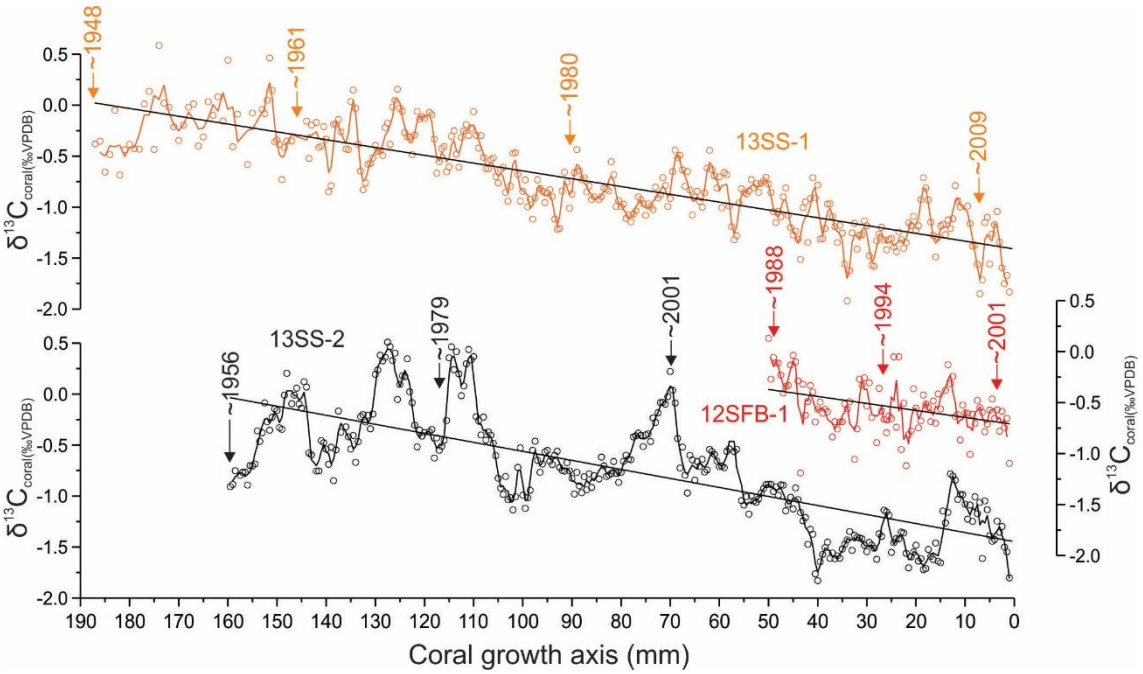

Figure 3. Skeletal $\delta^{13}C$ records for 13SS-1 (orange), 13SS-2 (black) and 12SFB-1 (red) colonies from the Rocas Atoll, South Atlantic Ocean (running average window width = 3). Arrows indicate values from ^{230}Th dating through sections of the coral growth axis.

4.1.1. Inter-annual variability

We applied Fourier transform analysis to quantitatively assess seasonal frequencies of the $\delta^{13}C$ time series of the three coral records (Fig. 4). Identification of frequencies likely to be annual were then compare to the growth rate estimated according to U-series ages and those available from the literature. Fourier transform analysis for coral 13SS-1 identified dominant peaks at the frequencies of 50, 8.2, 7.1 mm and weak peaks at the frequencies of 4.7, 3.3 and 2.4 mm (most probable annual cycles), which is closer to the estimated growth rate by U-series age. For colony 13SS-2, frequency peaks at intervals of 62.5, 18.0 (strong) and a weak peak at 4.3 mm (most probable annual cycle). For the

colony 12SFB-1, strong frequency peaks are observed at the intervals of 28.6, 5.3 and 3.6 mm, the later peak is consistent with the growth rate of 3.45year.mm^{-1}, based on U-series ages.

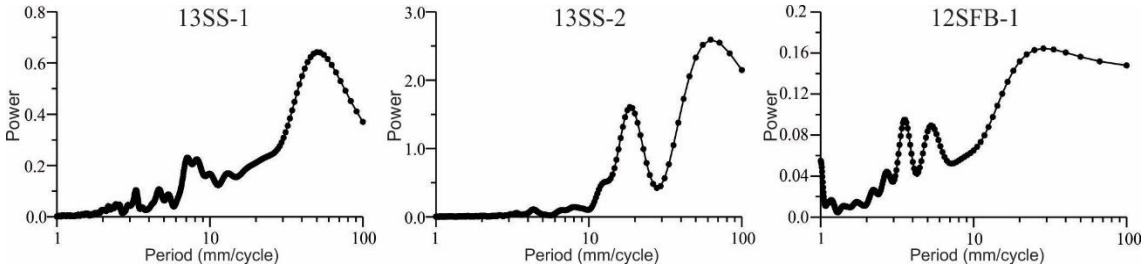

Figure 4. Fourier transform analysis of the $\delta^{13}C$ time series of the coral records 13SS-1 (a), 13SS-2 (b) and 12SFB-1 (c).

4.1.2. Long term variability

The decrease of the $\delta^{13}C$ in the three *S. stellata* records (Fig. 3) amounts to a depletion rate of about -0.0243 ± 0.0057 ‰.yr^{-1} for 12SFB-1($r = -0.40$, $p < 0.001$), -0.0208 ± 0.0007 ‰.yr^{-1} ($r = -0.83$, $p < 0.001$) for 13SS-1 and -0.0214 ± 0.0013 ‰.yr^{-1} ($r = -0.67$, $p < 0.001$) for 13SS-2.

4.2. Oxygen isotopes and Sr/Ca ratios

The coral $\delta^{18}O$ values range from −4.15 to −3.21‰, with a mean value of -3.68 ± 0.18‰ and variance of 0.03‰ in colony 13SS-1 (n = 295). Colony 12SFB-1 varied from −4.34 to −3.05 ‰, with mean value of -3.49 ± 0.26 ‰ and variance of 0.07‰ (n = 94). Sr/Ca ratios for the colony 13SS-1 range from 9.00 to 9.47 mmol/mol with a mean value of 9.26 ± 0.08 mmol/mol and variance of 0.006 mmol/mol (n = 295).

Both $\delta^{18}O$ and Sr/Ca ratios of 13SS-1 and $\delta^{18}O$ of 12SFB-1 lack coherent seasonal cycles and are strongly dominated by an inter-annual signal (Fig. 5). In 13SS-1, $\delta^{18}O$ and Sr/Ca are clearly correlated, but this covariation is dominated by multi-annual SST variability rather than seasonal cycles which are developed weakly at best. Within the resolution of the available age models no clear correlation of $\delta^{18}O$ data from the

specimens 13SS-1 and 12SFB-1 can be established, which might be associated to local signals of different tidal ponds at the Rocas Atoll.

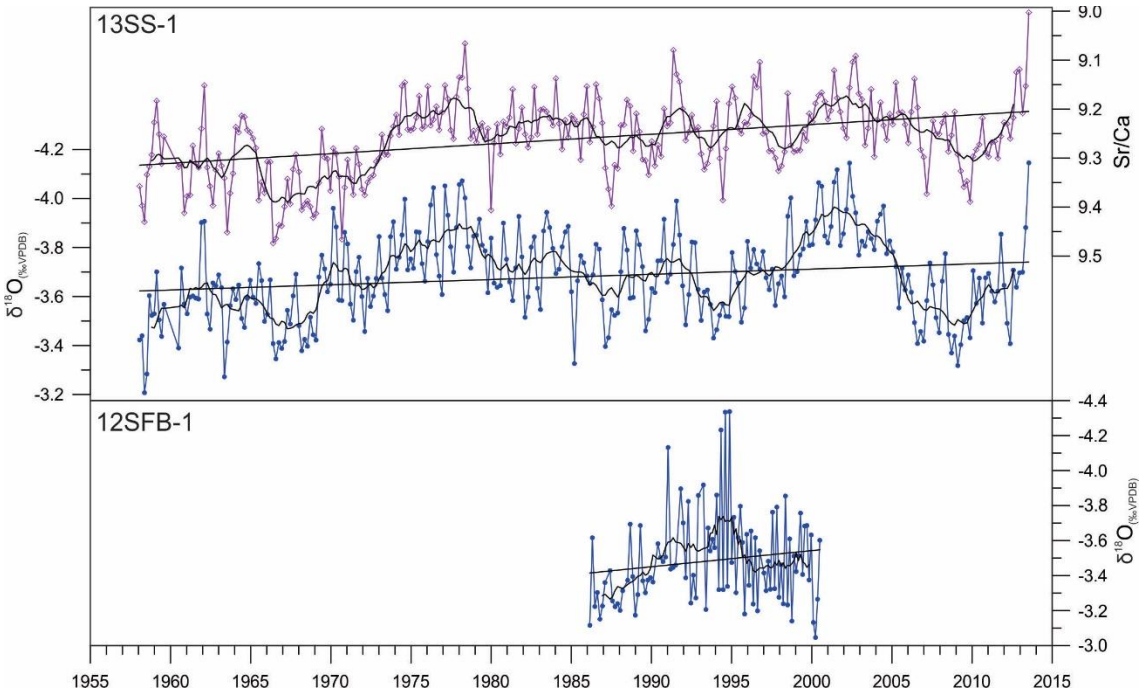

Figure 5. $\delta^{18}O$ and Sr/Ca data of colony 13SS-1 (top) and $\delta^{18}O$ data of 12SFB-1 (bottom). Sclerochronology based on the U-series age model. Running averages (11 data points averaged) are shown as black lines for the geochemical cycles.

5. Discussion

5.1. Seasonal variability of $\delta^{13}C$ and growth rate

Coral metabolism produces isotopic fractionation by respiration and photosynthetic activity by symbiotic zooxanthellae (Swart 1983a; McConnaughey 1989a, 1989b, among others). Since zooxanthellae photoactivity depends on light availability, $\delta^{13}C$ has been conventionally used as proxy for cloud cover (e.g. Fairbanks and Dodge 1979; Swart 1983a; Pätzold 1984; Swart et al. 1996; Fairbanks et al. 1997; Grottoli and Wellington 1999; Reynaud-Vaganay et al. 2001; Reynaud and Saint-Martin 2010). During photosynthesis zooxanthellae preferentially fix the ^{12}C, leading to ^{13}C enrichment in the

315 calcifying fluid and consequently higher $\delta^{13}C$ in coral aragonite (Swart 1983;
316 McConnaughey 1989).

317 The Fourier analysis indicated that the studied coral records have weak annual
318 variability and geochemical variance is dominated by lower frequency variance. The
319 equatorial location of the Rocas Atoll tends to be governed by stronger inter-annual
320 climate-related variability than seasonal variability compared to other sites. This is
321 evident in the three coral colonies that show weak peaks in the 4.7–2.5 mm/cycle range,
322 likely due to weak annual cycles, superimposed on stronger inter-annual variance (8.2
323 mm at the colony 13SS-1 and 18 mm at the colony13SS-2). Even the colony 12SFB-1, in
324 which carbon isotope cycles are compatible with U-series age, shows a dominant inter-
325 annual variance in the $\delta^{13}C$ record.

326 The growth rate for *S. stellata* for the Rocas Atoll was previously estimated by
327 Pinheiro et al. (2017) to be on average 6.8 ± 0.7 mm.year^{-1} using coralXDS software
328 (Helmle et al. 2002) – similar to the extension rate that can be deduced from some carbon
329 isotopic cycles in the coral records presented here. As discussed in section 4.1, the
330 comparison between the number of $\delta^{13}C$ cycles and U-series ages for colonies 13SS-1
331 and 13SS-2 (table 2) is compatible with die-off events in these colonies of *Siderastrea*,
332 probably associated environmental stress like SST anomalies. Multiple substantial growth
333 cessations through the coral life span, however, would be required to explain the gap in
334 time if the carbon isotope cycles were to be a reflection of seasonal environmental
335 variability. This seems unlikely given that there is little skeletal evidence of growth
336 cessation in the coral X-rays (except for the aforementioned growth anomaly in colony
337 13SS-2).

The weak signal revealed by the Fourier analysis at 2 to 4 mm is less than the annual extension porposed by Pinheiro et al (2017), but similar to values of linear extension rates (2.73 ± 0.35 mm.year^{-1}) for the same species at the coast of Bahia, Brazil, reported by Lins-de-Barros and Pires (2006), and specimens from this genus (*Siderastrea siderea*) from the coast of Florida, U.S.A. (Maupin et al. 2008; DeLong et al. 2011). These smaller extension rates (and carbon isotope fluctuations) underline that the seasonal $\delta^{13}C$ record in *S. stellata* from the Rocas Atoll is poorly defined and overprinted by larger multi-annual variability (Fig. 3). Consequently, the coral-based $\delta^{13}C$ records presented here do not permit annual correlation and the generation of high-fidelity stacked records for this species. However, the apparent non-linear growth of *S. stellata* seems to not obstruct the long-term trends toward increasingly depleted $\delta^{13}C$, which is explored below.

5.2. Potential sources of $\delta^{13}C$ variability at long term

While the short-term (intra-annual) variability of the three colonies is not well correlated, over multiple decades the $\delta^{13}C$ coral records show decreasing trends, which indicates a common environmental forcing. Since coral $\delta^{13}C$ has been interpreted as recording multiple environmental variables, we discuss each possibility below.

5.2.1. Changes in solar irradiation

As outlined in section 5.1., coral $\delta^{13}C$ is often associated with the photoactivity of the zooxanthellae (Swart 1983a). To produce the observed long-term decreasing trend in the coral $\delta^{13}C$ record, a reduction in solar irradiation would be expected.

Anthropogenic aerosols intensify the scattering and absorption of light (Ramanathan et al. 2001) and could potentially cause a reduction in the amount of solar irradiation reaching the coral. Measurements from 1960 to 1990 reported a decrease in solar irradiation of about 4 to 6% (Gilgen et al. 1998; Wild et al. 2005), leading to a global

362 dimming phenomenon (Wild et al. 2005), which could potentially trigger the decreasing
363 trend in coral $\delta^{13}C$.

364 However, a reversal from dimming to brightening conditions occurred after 1985,
365 causing an increasing in solar irradiation, possibly associated with reduction of aerosol
366 burden as a result of more effective clean-air regulations (Wild et al. 2005). This reversal
367 is not seen in the coral $\delta^{13}C$ record, thus, solar irradiance by itself cannot be the main
368 force governing the long-term $\delta^{13}C$ trend.

369 The total solar irradiance (TSI) for the period A.D. 1945–2007 (Fig. 7) was
370 reconstructed by using a physical model (http://vizier.cfa.harvard.edu/viz-bin/ VizieR?-
371 source=J/A+A/531/A6) (Vieira et al., 2011) in which no decreasing trend was observed
372 ($r = -0.09$, $p < 0.001$), thus TSI could not explain the observed changes in coral $\delta^{13}C$
373 through time.

374 *5.2.2. Heterotrophy*

375 The influence of zooplankton ingestion to the coral $\delta^{13}C$ through time also should
376 be considered. If the negative trend was caused by changes in the level of heterotrophy,
377 it is expected that the three investigated colonies have continuously increased the
378 ingestion of zooplankton (Grottoli and Wellington 1999). Zooplankton is an important
379 dietary component of corals, because it supplies nitrogen, phosphorus and other nutrients
380 that are not provided by the zooxanthellae (Sebens et al. 1998).

381 Colonies 13SS-1 and 13SS-2 were collected at the southern part of Rocas Atoll and
382 12SFB-1-1 was collected at the northwestern part of the atoll (Fig. 1). It thus would be
383 necessary to explain why colonies from distinct locations are increasing zooplankton
384 ingestion continuously through time: changes in phototrophic-heterotrophic strategies?
385 Plankton rich upwelling events? Decrease in water transparency and concurrent

386 inefficiency of zooxanthellae in supplying coral nutrients, leading to higher level of
387 heterotrophy? These potential explanations require much more data than are available to
388 fully explore, but they require invoking coincident physical and biological process
389 changes and are therefore not the most parsimonious of explanations for the decrease in
390 $\delta^{13}C$ common to all three specimens.

391 *5.2.3. Water depth*

392 Average coral $\delta^{13}C$ could be affected by water depth (Weber and Woodhead 1970).
393 Light intensity decreases with depth, reducing the photosynthesis activity of
394 zooxanthellae, which decreases the $\delta^{13}C$ signal in coral aragonite through a decreased
395 removal of ^{12}C for photosynthesis, as discussed above (Weber and Woodhead 1970).
396 However, when this mechanism was tested with 25 specimens of *S. stellata* from this site
397 (Mayal et al., 2009), no correlation between depth and $\delta^{13}C$ ($r = -0.29$, $p(a) > 0.05$, $n =$
398 28) was observed over 1 to 4 m water depth (Fig. 6). Additionally, assuming a linear age
399 model between U-series dates, we calculated the mean $\delta^{13}C$ in our three corals over the
400 common growth period of 2000-1986 and get the values −0.93 (13SS-1, 7 m depth), −0.60
401 (13SS-2, 7 m depth) and −0.54 (12SFB-1, 3 m depth), with no depth related trend. Thus,
402 we conclude that depth is not a major factor controlling $\delta^{13}C$ in these corals.

403

404

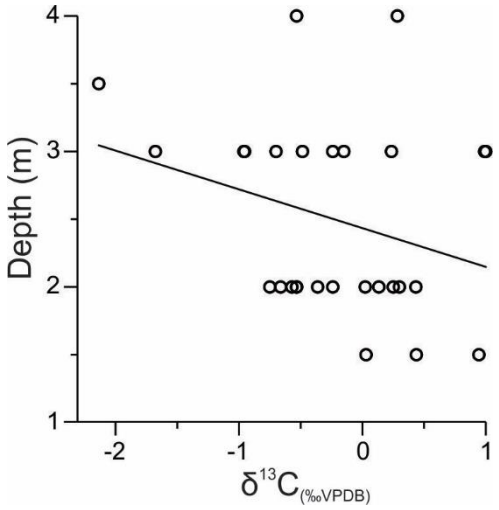

Figure 6. Cross plot of depth against mean $\delta^{13}C$ of different colonies of *S. stellata* analyzed by Mayal et al. (2009), showing no evident correlation.

5.2.4. Suess Effect and $\delta^{13}C$ of DIC

The decreasing rates observed in the corals of Rocas Atoll are similar to the reported trends for the $\delta^{13}C$ of atmospheric CO_2 over 1960-1990 (−0.023 to −0.029 ‰.yr^{-1}) (Keeling et al. 2010). Recently, decreasing trends on coral $\delta^{13}C$ for the Caribbean and North Atlantic (Swart et al. 2010; Hetzinger et al. 2016), Red Sea (Al-Rousan and Felis 2013) and Fiji (Swart et al. 2010; Dassié et al. 2013) have been reported. These authors attributed the decreasing trend to decreasing $\delta^{13}C$ values of the DIC, ultimately governed by changes in the carbon isotopic composition of atmospheric CO_2, caused by increasing anthropogenic CO_2 emissions, known as the Suess Effect (Keeling 1979).

Most of the coral records used to assess the Suess Effect date up to 1990 (Swart et al. 2010; Dassié et al. 2013) and these records show differences in detail, but generally exhibit a steepening downward slope between 1960-1990. The data presented for the $\delta^{13}C$ based on coral archives for the South Atlantic Ocean have $\delta^{13}C$ trends similar to those from the North Atlantic Ocean (−0.019 ‰.yr^{-1}) between 1960-1990 (Swart et al. 2010), which are comparatively higher than the coral $\delta^{13}C$ trends from the Pacific Ocean reported

by Swart et al. (2010) (−0.0066 ‰.yr^{-1}) and Dassié et al. (2013) (−0.014 ‰·yr^{-1}), and from the Indian Ocean (−0.0057 ‰.yr^{-1} (Al-Rousan and Felis 2013)) for the same period.

Coral-based records of the same genus of this study (*Siderastrea*) were reported from Florida for the period of 1960-1994, with a decreasing rate for the $\delta^{13}C$ values varying from −0.0274 to –0.0289 ‰.yr^{-1} (Swart et al. 2010) and Dominica, for the period between 1960-2000 and presented a $\delta^{13}C$ decreasing rate of −0.0217 ‰.yr^{-1} (Swart et al. 2010), equivalent to values reported for *S. stellata* from the Rocas Atoll. Table 2 summarizes published coral $\delta^{13}C$ trends in different locations.

Table 3. Comparison of coral $\delta^{13}C$ trends from Rocas Atoll and other regions.

Data set	Location	Coral	Period	$\delta^{13}C_{(‰VPDB)}$				Decreasing rate (‰.yr^{-1})
				average	max	min	range	
12SFB-1	South Atlantic	*S. stellata*	1988–2001	−0.53 (±0.26)	0.13	−1.19	1.32	−0.0243
13SS-1	South Atlantic	*S. stellata*	1948–2013	−0.76 (±0.55)	0.58	−2.76	3.34	−0.0208
13SS-2	South Atlantic	*S. stellata*	1956–2013	−0.75 (±0.47)	0.51	−2.06	2.57	−0.0214
Dassié et al (2013)	Fiji	*Porites sp.*	1781–2001	–	–	–	–	−0.0052
Dassié et al (2013)	Fiji	*Porites sp.*	1960–1990	–	–	–	–	−0.014
Swart et al (2010)	Pacific Ocean	Multiple	1960–1999	–	–	–	–	−0.0066
Swart et al (2010)	Indian Ocean	Multiple	1900–1990	–	–	–	–	−0.0057
Wei et al. (2009)	GBR	*Porites sp.*	1950–2004	–	–	–	–	−0.028
Swart et al (2010)	North Atlantic	Multiple	1960–1990	–	–	–	–	−0.019
Al-Rousan and Felis (2013)	Gulf of Aqaba	*Porites*	1974–2004	–	–	–	–	−0.029
*CO_2 Ascension Island	South Atlantic	–	1992-2014	−8.08 (±0.18)	−7.48	−8.87	1.34	−0.027
**DIC	Tropical Atlantic		1991-2003	1.77 (±0.82)	1.91	1.56	0.34	−0.013

*Measurements of carbon stable isotope for the atmospheric CO_2 from Ascension Island and **DIC from Tropical Atlantic is display for comparison.

$\delta^{13}C$ data of atmospheric CO_2 at the interval of 1992 to 2014 from the oceanic Ascension Island (Fig. 6), a location in the tropical South Atlantic Ocean with similar conditions to Rocas Atoll yielded a decreasing trend of −0.027 ‰yr^{-1}, slightly higher than the coral records presented here (table 3).

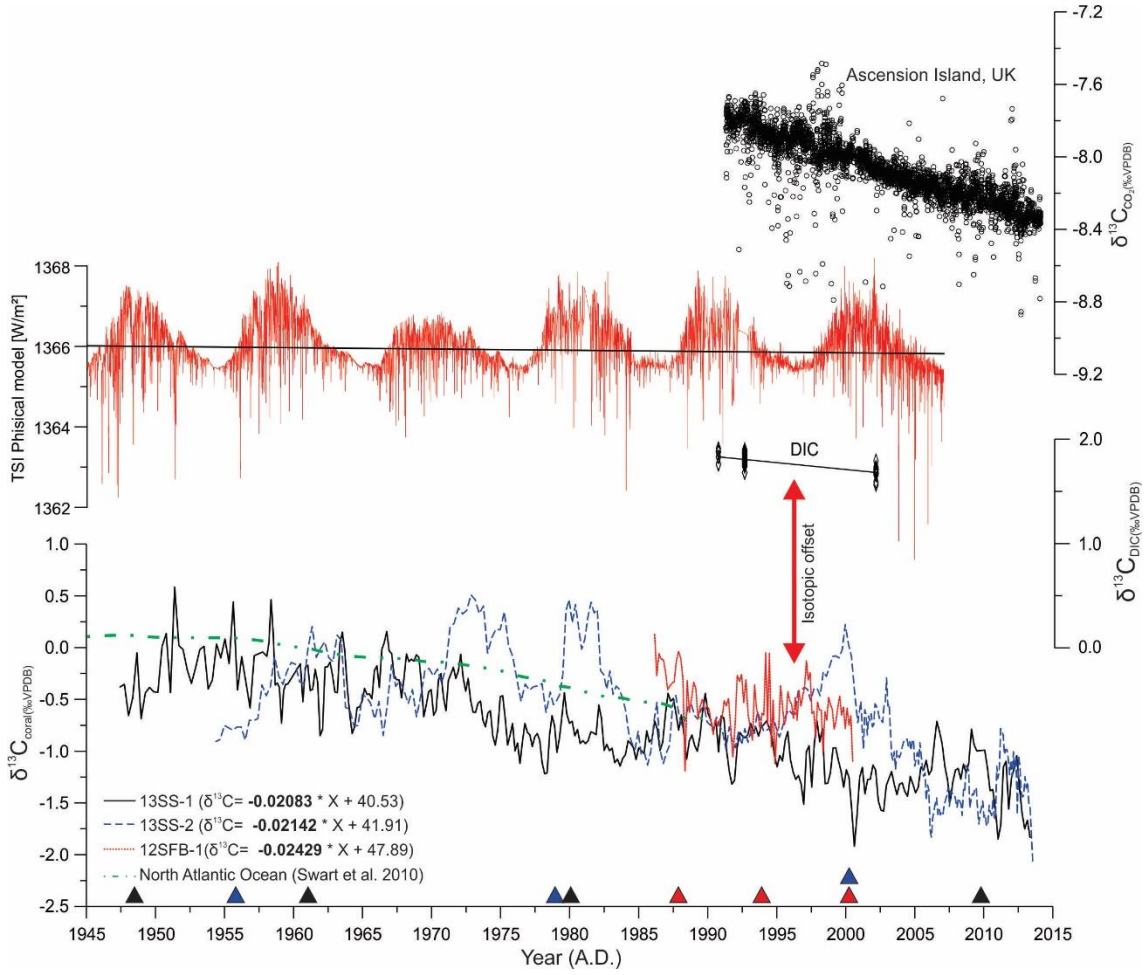

439

440 **Figure 7. Evolution of the $\delta^{13}C$ of colonies 13SS-1, 13SS-2 and 12SFB-1 through time,**
441 **together with the data of the coral $\delta^{13}C$ trend for the North Atlantic Ocean published by**
442 **Swart et al. (2010).Time series of the CO_2 carbon isotope from Ascension Island, UK for the**
443 **period from 1992 to 2014 and DIC from the Tropical Atlantic Ocean (data compiled from**
444 **Schmittner et al. (2013)) and Total Solar Irradiance from 1945 to 2007 are plotted together**
445 **for comparison. Colored triangles represent age tie points (U-series) used for age model of**
446 **each colony, 13SS-1 (black); 13SS-2 (blue) and 12SFB-1 (red).**

447 Carbon stable isotope data for DIC from Tropical Atlantic (latitude varying from 8
448 to -9), compiled from Schmittner et al. (2013) for the period of 1991 to 2003, show a
449 decreasing trend of -0.013 ‰.yr^{-1}, whereas, for a global estimation, Gruber et al. (1999)
450 proposed a $\delta^{13}C$ decrease rate of the surface oceanic DIC of approximately -0.018 ‰.yr^{-1}
451 from 1985 to 1995.

452 The coral records presented here show slightly higher trends compared to
453 Schmittner et al (2013) but closer to the trend from the Gruber global compilation. The
454 carbon isotopic composition of DIC can be site specific (Quay et al 2003) which could
455 explain different trends between $\delta^{13}C$ of corals from Rocas and global DIC estimates.
456 This difference suggests that the coral record from the Rocas Atoll tracks changes in the
457 isotopic signature of local DIC.

458 The offset between the $\delta^{13}C$ from coral records and the surface DIC from this part
459 of the tropical Atlantic is approximately 2.3‰ (Fig. 7) which can be attributed to the
460 prevailing biological fractionation during coral biomineralisation. The primary long-term
461 signal from multiple records nevertheless is visible as a consistent $\delta^{13}C$ decreasing trend
462 thus imaging the Suess Effect. This successful detection of the Suess Effect highlights the
463 possibility of tracking changes in the $\delta^{13}C$ of the oceanic DIC and eventually, correlation
464 with $\delta^{13}C$ composition of the atmospheric CO_2 using *S. stellata*.

465 **6. Conclusions**

466 $\delta^{13}C$ time series of three colonies of *S. stellata* from the tropical South Atlantic
467 Ocean have been presented. The $\delta^{13}C$ signal is mostly dominated by inter-annual
468 variation, with weak annual signals. The latter are probably controlled by the solar
469 irradiation conditions at the tropical South Atlantic that influence zooxanthellae
470 photosynthesis activity.

471 $\delta^{13}C$ showed a consistent decadal trend toward negative values, with a decreasing
472 rate varying from −0.0208 to −0.0243 similar to rates expected from the Suess Effect.
473 These trends are also very similar to the global estimates for changes in carbon isotopic
474 composition of sea-surface DIC, suggesting that the $\delta^{13}C$ coral-based records from the

Rocas Atoll presented in this study are directly influenced by the $\delta^{13}C$ signature of local DIC.

This study confirms that multiple $\delta^{13}C$ coral-based records can detect long-term changes in the $\delta^{13}C_{DIC}$ of the ocean and, ultimately, identify changes in the $\delta^{13}C$ of the atmospheric CO_2, contributing to the understanding of the recent carbon cycle disturbances within the atmosphere-ocean system during the Anthropocene epoch.

Acknowledgments

NSP acknowledges the National Counsel of Technological and Scientific Development (CNPq) for a Post-Doctoral Scholarship Proc. nº 150405/2015-4. We thank the chief of the Biological Reserve of Rocas Atoll, Maurizélia de Brito Silva and the field team Tiago Albuquerque, Miguel Miranda, Mirella B. Costa and Eduardo Macêdo, for the great assistance in this study. We thank Gilsa Santana, Vilma Sobral (NEG-LABISE, Brazil) and Bo Petersen (University of Copenhagen) for assisting in stable isotope measurements. We are thankful for the critical and constructive comments of the anonymous reviewers. U-Th dating was supported by grants from Ministry of Science and Technology (MOST) (104-2119-M-002-003, 105-2119-M-002-001 to C.-C.S.) and the National Taiwan University (105R7625 to C.-C.S.). This manuscript is the scientific contribution nº XXX of the NEG-LABISE, UFPE, a contribution of the Reef Ecosystems Working Group of the INCT Ambientes Marinhos Tropicais (InctAmbTropic – CNPq #565.054/2010-4), and represents contribution XXXX of the University of Maryland Center for Environmental Science.

References

Al-Rousan S, Felis T (2013) Long-term variability in the stable carbon isotopic composition of Porites corals at the northern Gulf of Aqaba, Red Sea. Palaeogeogr Palaeoclimatol Palaeoecol 381–382:1–14

Andres RJ, Boden TA, Marland G (2013) Annual Fossil-Fuel CO2 Emissions: Global Stable Carbon Isotopic Signature, (Carbon Dioxide Information Analysis Center,

Oak Ridge National Laboratory, US Department of Energy, Oak Ridge, Tenn., USA, 2013).

Cheng H, Edwards RL, Shen C, Polyak VJ, Asmerom Y, Woodhead J, Hellstrom J, Wang Y, Kong X, Spötl C, Wang X, Alexander EC (2013) Improvements in 230 Th dating , 230 Th and 234 U half-life values , and U – Th isotopic measurements by multi-collector inductively coupled plasma mass spectrometry. Earth Planet Sci Lett 371–372:82–91

Corrège T (2006) Sea surface temperature and salinity reconstruction from coral geochemical tracers. Palaeogeogr Palaeoclimatol Palaeoecol 232:408–428

Dassié E, Lemley G, Linsley B (2013) The Suess effect in Fiji coral δ13C and its potential as a tracer of anthropogenic CO2 uptake. Palaeogeogr Palaeoclimatol Palaeoecol 370:30–40

DeLong KL, Flannery JA, Maupin CR, Poore RZ, Quinn TM (2011) A coral Sr/Ca calibration and replication study of two massive corals from the Gulf of Mexico. Palaeogeogr Palaeoclimatol Palaeoecol 307:117–128

DeLong KL, Quinn TM, Taylor FW (2007) Reconstructing twentieth-century sea surface temperature variability in the southwest Pacific: A replication study using multiple coral Sr/Ca records from New Caledonia. Paleoceanography 22:PA4212

DeLong KL, Quinn TM, Taylor FW, Shen C-C, Lin K (2013) Improving coral-base paleoclimate reconstructions by replicating 350years of coral Sr/Ca variations. Palaeogeogr Palaeoclimatol Palaeoecol 373:6–24

Deng W, Chen X, Wei G, Zeng T, Zhao J (2017) Decoupling of coral skeletal 13C and solar irradiance over the past millennium caused by the oceanic Suess effect. Paleoceanography 32:161–171

Dettinger MD, Ghil M, Strong CM, Weibel W, Yiou P (1995) Software expedites singular-spectrum analysis of noisy time series. Eos, Trans Am Geophys Union 76:12–21

Druffel ERM, Benavides LM (1986) Input of excess CO2 to the surface ocean based on 13C/12C ratios in a banded Jamaican sclerosponge. Nature 321:58–61

Fairbanks RG, Dodge RE (1979) Annual periodicity of the the 18O/16O and 13C/12C and ratios in the coral Montastrea annularis. Geochim Cosmochim Acta 43:1009–1020

Fairbanks RG, Evans MN, Rubenstone JL, Mortlock RA, Broad K, Moore MD, Charles CD (1997) Evaluating climate indices and their geochemical proxies measured in corals. Coral Reefs 16:S93–S100

Felis T, Pätzold J, Loya Y, Fine M, Nawar AH, Wefer G (2000) A coral oxygen isotope record from the northern Red Sea documenting NAO, ENSO, and North Pacific teleconnections on Middle East climate variability since the year 1750. Paleoceanography 15:679–694

Friedli H, Lötscher H, Oeschger H, Siegenthaler U, Stauffer B (1986) Ice core record of the 13C/12C ratio of atmospheric CO2 in the past two centuries. Nature 324:237–238

Gagan MK, Chivas AR, Isdale PJ (1994) High-resolution isotopic records from corals using ocean temperature and mass-spawning chronometers. Earth Planet Sci Lett 121:549–558

Gherardi DFM, Bosence D (2001) Composition and community structure of the coralline algal reefs from Atol das Rocas, South Atlantic, Brazil. Coral Reefs 19:205–219

Ghil M, Allen MR, Dettinger MD, Ide K, Kondrashov D, Mann ME, Robertson AW, Saunders A, Tian Y, Varadi F, Yiou P (2002) Advanced spectral methods for climatic time series. Rev Geophys 40:1–41

Gilgen H, Wild M, Ohmura A, Gilgen H, Wild M, Ohmura A (1998) Means and Trends of Shortwave Irradiance at the Surface Estimated from Global Energy Balance Archive Data. J Clim 11:2042–2061

Grottoli a. G, Wellington GM (1999) Effect of light and zooplankton on skeletal δ 13 C values in the eastern Pacific corals Pavona clavus and Pavona gigantea. Coral Reefs 18:29–41

Gruber N, Keeling CD, Bacastow RB, Guenther PR, Lueker TJ, Wahlen M, Meijer HAJ, Mook WG, Stocker TF (1999) Spatiotemporal patterns of carbon-13 in the global surface oceans and the oceanic Suess effect. Global Biogeochem Cycles 13:307–335

Guilderson TP, Fairbanks RG, Rubenstone JL (2001) Tropical Atlantic coral oxygen isotopes: glacial–interglacial sea surface temperatures and climate change. Mar Geol 172:75–89

Helmle KP, Kohler KE, Dodge RE (2002) Relative Optical Densitometry and The Coral X-radiograph Densitometry System: CoralXDS.

Keeling CD (1979) The Suess effect: 13Carbon-14Carbon interrelations. Environ Int 2:229–300

Keeling R, Piper S, Bollenbacher A, Walker S (2010) In Trends: A Compendium of Data on Global Change. (Carbon Dioxide Information Analysis Center, Oak Ridge National Laboratory, US Department of Energy., Oak Ridge, Tenn., USA, 2010).

Kikuchi RKP, Leão ZMAN (1997) Rocas (Southwestern Equatorial Atlantic, Brazil): An Atoll Built Primarily By Coralline Algae. 731–736

Knutson DW, Buddemeier RW, Smith S V (1972) Coral chronometers: seasonal growth bands in reef corals. Science 177:270–2

Leder JJ, Swart PK, Szmant a. M, Dodge RE (1996) The origin of variations in the isotopic record of scleractinian corals: I. Oxygen. Geochim Cosmochim Acta 60:2857–2870

Leder JJ, Szmant AM, Swart PK (1991) The effect of prolonged “bleaching” on skeletal banding and stable isotopic composition in Montastrea annularis Preliminary observations. Coral Reefs 10:19–27

Lins-de-Barros M, Pires DO (2007) COMPARISON OF THE REPRODUCTIVE STATUS OF THE SCLERACTINIAN CORAL SIDERASTREA STELLATA THROUGHOUT A GRADIENT OF 20º OF LATITUDE. Brazilian J Oceanogr

586 55:67–69

587 Lins-de-Barros MM, Pires DO (2006) Aspects of the life history of Siderastrea stellata
588 in the tropical Western Atlantic, Brazil. Invertebr Reprod Dev 49:237–244

589 Linsley BK, Dunbar RB, Wellington GM, Mucciarone DA (1994) A coral-based
590 reconstruction of Intertropical Convergence Zone variability over Central America
591 since 1707. J Geophys Res 99:9977–9994

592 Maupin CR, Quinn TM, Halley RB (2008) Extracting a climate signal from the skeletal
593 geochemistry of the Caribbean coral Siderastrea siderea. Geochemistry, Geophys
594 Geosystems 9:n/a-n/a

595 Mayal EM, Sial AN, Ferreira VP, Fisner M, Pinheiro BR (2009) Thermal stress
596 assessment using carbon and oxygen isotopes from Scleractinia, Rocas Atoll,
597 northeastern Brazil. Int Geol Rev 51:166–188

598 McConnaughey T (1989a) 13C and 18O isotopic disequilibrium in biological
599 carbonates: II. In vitro simulation of kinetic isotope effects. Geochim Cosmochim
600 Acta 53:163–171

601 McConnaughey T (1989b) 13C and 18O isotopic disequilibrium in biological
602 carbonates: I. Patterns. Geochim Cosmochim Acta 53:151–162

603 McConnaughey TA (2003) Sub-equilibrium oxygen-18 and carbon-13 levels in
604 biological carbonates: carbonate and kinetic models. Coral Reefs 22:316–327

605 Moses CS, Swart PK, Dodge RE (2006) Calibration of stable oxygen isotopes in
606 Siderastrea radians (Cnidaria:Scleractinia): Implications for slow-growing corals.
607 Geochemistry, Geophys Geosystems 7:1–14

608 Nozaki Y, Rye DM, Turekian KK, Dodge RE (1978) A 200 year record of carbon-13
609 and carbon-14 variations in a Bermuda coral. Geophys Res Lett 5:825–828

610 Orr JC, Maier-Reimer E, Mikolajewicz U, Monfray P, Sarmiento JL, Toggweiler JR,
611 Taylor NK, Palmer J, Gruber N, Sabine CL, Le Quéré C, Key RM, Boutin J (2001)
612 Estimates of anthropogenic carbon uptake from four three-dimensional global
613 ocean models. Global Biogeochem Cycles 15:43–60

614 Pätzold J (1984) Growth rhythms recorded in stable isotopes and density bands in the
615 reef coral Porites lobata (Cebu, Philippines). Coral Reefs 3:87–90

616 Pereira NS, Manso VAV, Macedo RJA, Dias JMA, Silva AMC (2013) Detrital
617 carbonate sedimentation of the Rocas Atoll, South Atlantic. An Acad Bras Cienc
618 85:57–72

619 Pereira et al 2010 (2010) Mapeamento Geomorfológico e Morfodinâmica do
620 Geomorphological Mapping and Morphodynamic of Rocas atoll , South Atlantic.
621 10:331–345

622 Pinheiro BR, Pereira NS, Agostinho PGF, Montes MJF (2017) Population dynamics of
623 Siderastrea stellata Verrill , 1868 from Rocas Atoll , RN : implications for
624 predicted climate change impacts at the only South Atlantic atoll. Ann Brazilian
625 Acad Sci 89:873–884

626 Quay PD, Tilbrook B, Wong CS (1992) Oceanic Uptake of Fossil Fuel CO2: Carbon-13
627 Evidence. Science 256:74–9

Ramanathan V, Crutzen PJ, Kiehl JT, Rosenfeld D (2001) Aerosols, Climate, and the Hydrological Cycle. Science (80-) 294:

Reynaud-vaganay SY, Juillet-leclerc A, Jaubert J, Gattuso J (2001) Effect of light on skeletal δ13C and δ18O, and interaction with photosynthesis, respiration and calcification in two zooxanthellate scleractinian corals. Palaeogeogr Palaeoclimatol Palaeoecol 175:393–404

Reynaud S, Saint-martin A (2010) Light effects on the isotopic fractionation of skeletal oxygen and carbon in the cultured zooxanthellate coral , Acropora: implications for coral-growth rates. Biogeociences 7:893–906

Sebens KP, Grace SP, Helmuth B, Maney EJ, Miles JS (1998) Water flow and prey capture by three scleractinian corals, Madracis mirabilis, Montastrea cavernoss and Porites porites in a field enclosure. Mar Biol 131:347–360

Shen C-C, Li K-S, Sieh K, Natawidjaja D, Cheng H, Wang X, Edwards RL, Lam DD, Hsieh Y-T, Fan T-Y, Meltzner AJ, Taylor FW, Quinn TM, Chiang H-W, Kilbourne KH (2008a) Variation of initial 230Th/232Th and limits of high precision U–Th dating of shallow-water corals. Geochim Cosmochim Acta 72:4201–4223

Shen C, Li K, Sieh K, Natawidjaja D, Cheng H, Wang X, Edwards RL, Dinh D, Hsieh Y, Fan T, Meltzner AJ, Taylor FW, Quinn TM, Chiang H, Kilbourne KH (2008b) Variation of initial 230 Th / 232 Th and limits of high precision U – Th dating of shallow-water corals. 72:4201–4223

Shen C, Wu C, Cheng H, Edwards RL, Hsieh Y, Gallet S, Chang C, Li T (2012) High-precision and high-resolution carbonate 230 Th dating by MC-ICP-MS with SEM protocols. Geochim Cosmochim Acta 99:71–86

Spötl C, Vennemann TW (2003) Continuous-flow isotope ratio mass spectrometric analysis of carbonate minerals. Rapid Commun Mass Spectrom 17:1004–6

Sun D, Su R, McConnaughey TA, Bloemendal J (2008) Variability of skeletal growth and δ13C in massive corals from the South China Sea: Effects of photosynthesis, respiration and human activities. Chem Geol 255:414–425

Swart P (1983a) Carbon and oxygen isotope fractionation in scleractinian corals: a review. Earth-Science Rev 19:51–80

Swart P, Leder J, Szmant A, Dodge R (1996) The origin of variations in the isotopic record of scleractinian corals: II. Carbon. Geochim Cosmochim Acta 60:2871–2885

Swart PK (1983b) Carbon and Oxygen Isotope Fractionation in ScleracUnian Corals : a Review. 19:

Swart PK, Elderfield H, Greaves MJ (2002) A high-resolution calibration of Sr/Ca thermometry using the Caribbean coral Montastraea annularis. Geochemistry, Geophys Geosystems 3:1–11

Swart PK, Greer L, Rosenheim BE, Moses CS, Waite AJ, Winter a., Dodge RE, Helmle K (2010) The 13 C Suess effect in scleractinian corals mirror changes in the anthropogenic CO 2 inventory of the surface oceans. Geophys Res Lett 37:n/a-n/a

671 Swart PK, Grottoli a. (2003) Proxy indicators of climate in coral skeletons: a
672 perspective. Coral Reefs 22:313–315

673 Ullmann C V., Böhm F, Rickaby REM, Wiechert U, Korte C (2013) The Giant Pacific
674 Oyster (Crassostrea gigas) as a modern analog for fossil ostreoids: Isotopic (Ca,
675 O, C) and elemental (Mg/Ca, Sr/Ca, Mn/Ca) proxies. Geochemistry, Geophys
676 Geosystems 14:4109–4120

677 Weber J, Woodhead P (1970) Carbon and oxygen isotope fractionation in the skeletal
678 carbonate of reef-building corals. Chem Geol 6:93–117

679 Weber JN (1973) Incorporation of strontium into reef coral skeletal carbonate. Geochim
680 Cosmochim Acta 37:2173–2190

681 Weber JN, Woodhead PMJ (1972) Temperature dependence of oxygen-18
682 concentration in reef coral carbonates. J Geophys Res 77:463–473

683 Wei G, McCulloch MT, Mortimer G, Deng W, Xie L (2009) Evidence for ocean
684 acidification in the Great Barrier Reef of Australia. Geochim Cosmochim Acta
685 73:2332–2346

686 Wild M, Gilgen H, Roesch A, Ohmura A, Long CN, Dutton EG, Forgan B, Kallis A,
687 Russak V, Tsvetkov A (2005) From Dimming to Brightening: Decadal Changes in
688 Solar Radiation at Earth's Surface. Science (80-) 308:

689